SWITCHED RELUCTANCE MOTOR DRIVES

Switched reluctance motor (SRM) drives are relatively new to the rapidly developing variable speed drives market. They are variable speed drives that have a simple construction, wide speed range, good energy efficiency, high torque to inertia ratio, and high torque to power density ratio. The simple structure of SRMs will likely make them less expensive than the equivalent variable speed drives in mass production. SRMs are flexible in that they can operate as four-quadrant drives with independent control of speed and torque over a wide speed range. Their wide torque and speed range eliminates the need for expensive and troublesome mechanical gears and transmissions. Figure 1 shows the selection of SRMs with power ranging from 100 W to 75 kW and with a speed range of 250 rpm to 30,000 rpm (1).

HISTORICAL BACKGROUND

The SRM is the modern version of the electromagnetic engine, which dates back to the late 1830s. The modern era of SRM development started in 1972 when the SRM was patented by Bedford (2,3). The SRM received considerable attention upon the completion of some exemplary work at the Universities of Leeds and Nottingham in the 1980s (4–6). This research spurred a series of research activities all over the world, especially in Europe and in the United States, resulting in several publications, patents, and applications (1), as illustrated in Fig. 2. Even after almost 30 years of research involving the SRM, which appears to be the simplest of all machines, there remain some critical issues that need further study.

BASIC PRINCIPLES OF OPERATION

SRMs are structurally similar to variable reluctance stepper motors, but they differ in the following ways:

- stator phase currents are switched based on the rotor position feedback
- the SRM is designed to operate efficiently for a wide range of speed.

An SRM has salient poles on both stator and rotor. It has concentrated windings only on the stator and no windings on the rotor. Windings on the diametrically opposite stator poles are connected in series. Figure 3 shows a typical 8/6 SRM. Currents in the stator windings are switched on and off in accordance with the rotor position feedback.

The basic principle of operation of a SRM is like that of any other reluctance motor—torque is produced by the tendency of the rotor to align itself to the minimum reluctance position. Because this is independent of the direction of the current in the stator windings, the power converter circuit can be simplified. The radial magnetic attraction that operates the SRM is about ten times larger than the circumferential forces that operate an induction motor. The torque–speed characteristics of an SRM replicate a conventional dc machine characteristics under fixed firing switching strategy.

Flux/Current/Position Relationship

Typical characteristics of variation in the flux linkage with current at different rotor positions are shown in the Fig. 4.

Effect of Saturation

When the stator current is very high, the effect of saturation is typical in doubly salient machines, and a complete knowledge of saturation is required to design the machine. The two types of saturation to be considered are local and bulk saturation. Local saturation occurs when the poles are just approaching or just leaving the overlapping position (i.e., under partially aligned conditions). This leads to tip saturation because of flux fringing. Bulk saturation occurs in the fully aligned position resulting in a large loss of torque produced by the machine.

Saturation improves the ratio of mechanical energy to the stored magnetic field energy for a given input energy. In a complete working stroke, let the total converted electromechanical energy be W_m and the energy returned by the motor to the external circuit be W_r, then the energy ratio is defined as $W_m/(W_m + W_r)$. Comparing Figs. 5(a) and 5(b), it can be shown that in a saturating motor like SRM the energy ratio is greater (7).

It is important to note that the torque developed by doubly salient machines under saturated conditions is almost twice that found under unsaturated conditions. These nonlinear characteristics, which are the result of saturation, are very important in predicting the performance of the machine.

Voltage Equation. The stator voltage equation can be written as

$$V = Ri + d\Psi/dt \quad (1)$$

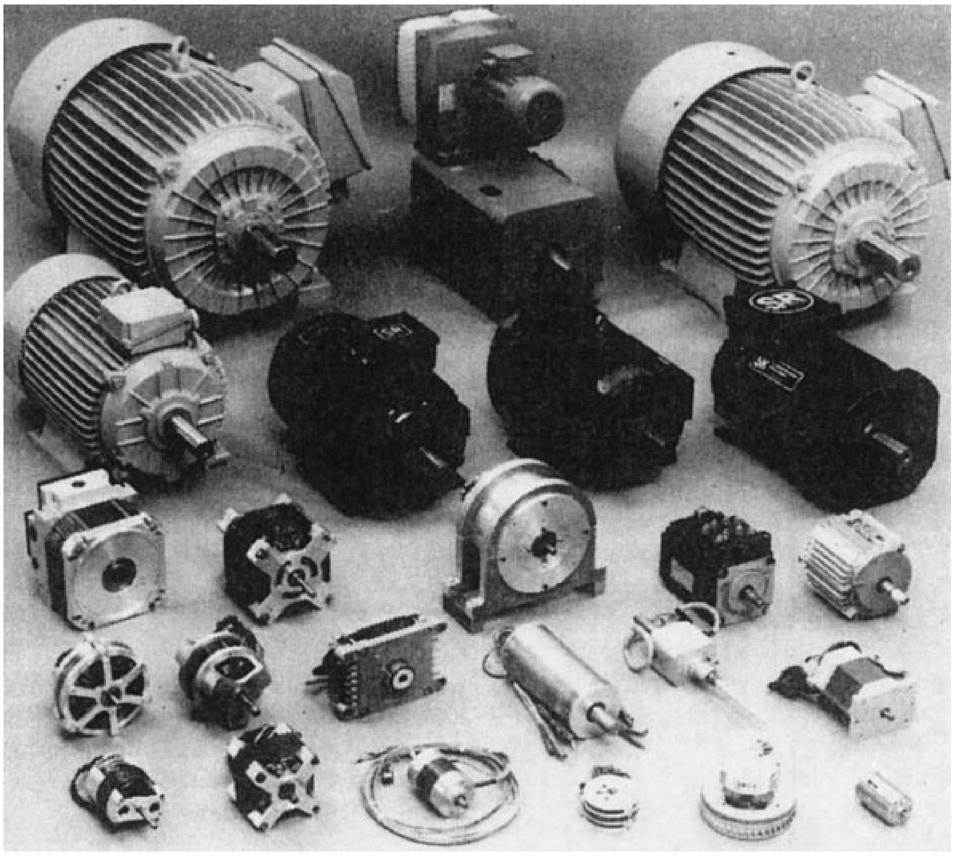

Figure 1. Selection of SRMs. (Courtesy of Emerson Motor divisions.

where V is the dc bus voltage, R is the winding resistance, i is instantaneous phase current, and ψ is the flux linking the stator coil (5). Expanding Eq. (1) based on the dependence of flux on stator current and rotor position

$$V = Ri + L(di/dt) + i(dL/d\theta)\omega \tag{2}$$

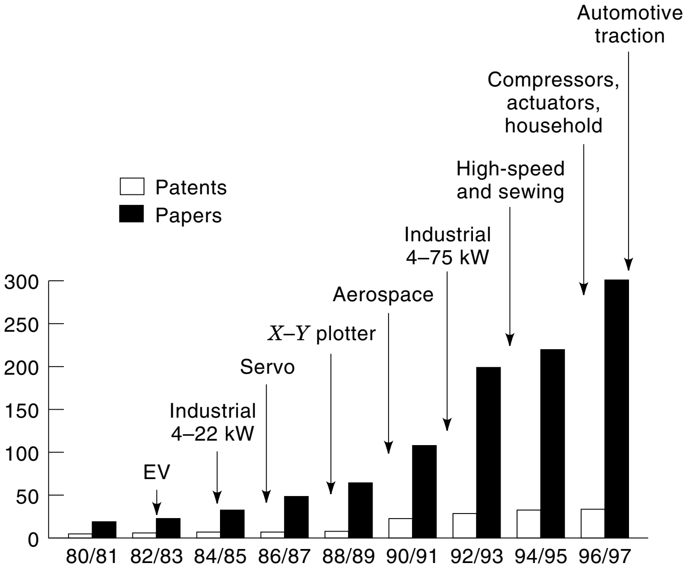

Figure 2. Approximate number of publications, patents, and applications.

where L is the inductance, ω is the rotor speed, and θ represents the rotor angular position. Neglecting magnetic nonlinearity

$$\Psi = Li \tag{3}$$

The third term in Eq. (2) is the motional electromotive force (emf), which depends on the phase current and the rate of change of inductance with rotor position. Figure 6 shows the ideal case variation of inductance with position.

Energy Flow. Multiplying Eq. (2) by i on both sides and neglecting the resistance term, we get

$$Vi = d/dt\left(\frac{1}{2}Li^2\right) + (i^2/2)(dL/d\theta)\omega \tag{4}$$

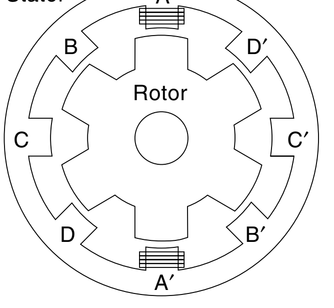

Figure 3. Typical 8/6 SRM.

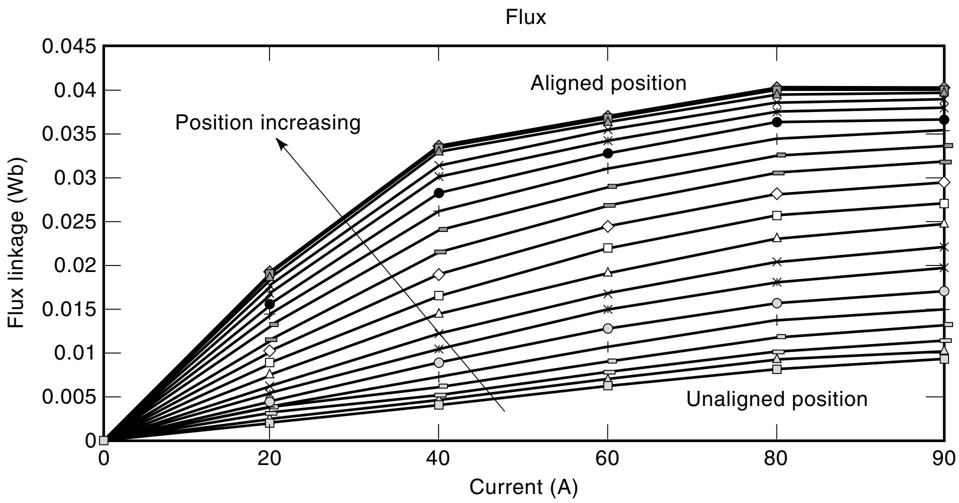

Figure 4. Flux/current/position curves.

The first term of Eq. (4) is the stored magnetic energy, and the second term is the mechanical power output. From Eq. (4) it can be interpreted that by simply controlling the switching instants of the stator current, a four-quadrant operation of the SRM can be easily achieved.

Torque Equation. Co-energy can be used to calculate the torque as follows:

$$T(\theta, i) = \partial W'(\theta, i)/\partial\theta \tag{5}$$

where co-energy is defined as

$$W'(\theta, i) = \int_0^{i} \Psi(\theta, i)\, di \tag{6}$$

Based on the simplified magnetic model neglecting saturation (3), Eq. (6) can be reduced to

$$T(\theta, i) = (i^2/2)(dL/d\theta) \tag{7}$$

Torque-Speed Curve. As shown in the Fig. 7, the torque–speed plane can be basically divided into three regions. The torque remains constant below the base speed. The base speed is defined as the highest speed at which maximum current can be supplied to the motor at rated voltage with fixed firing angles. Base speed is the basically the lowest speed at which maximum power can be extracted and the highest speed for maximum torque. In the constant torque, low-speed region where the motional emf is small, the current must be limited by some form of current control. This region offers the flexibility of current control to obtain the desired performance

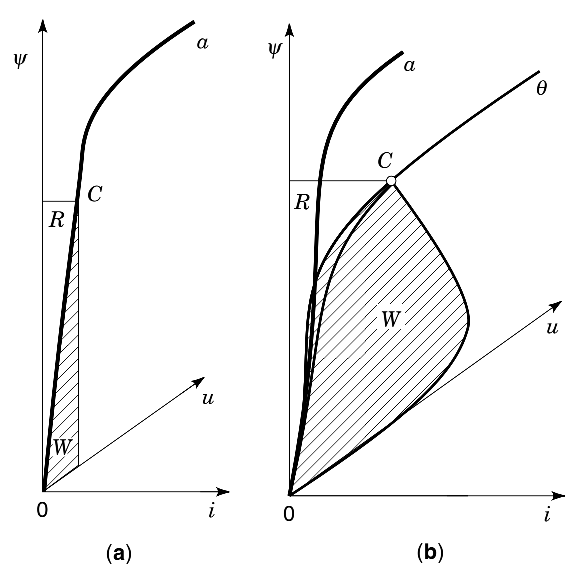

Figure 5. (a) Energy exchanges in one complete working cycle—linear case. (b). Energy exchanges in one complete working cycle—saturated case.

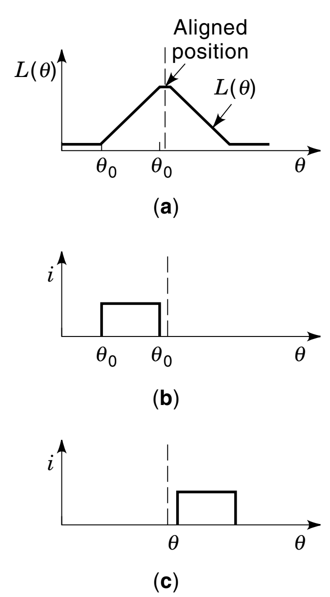

Figure 6. Inductance profile and phase current—ideal case. (a) Inductance profile, (b) phase current for motoring operation, and (c) phase current for generating operation.

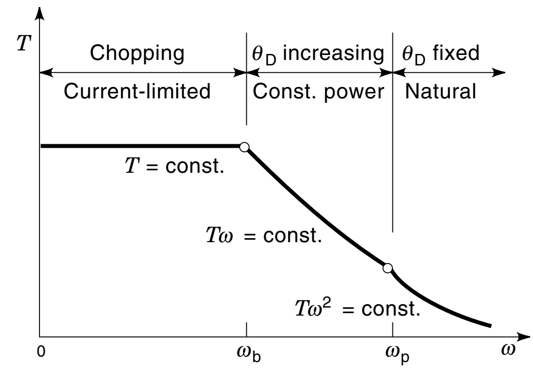

Figure 7. Torque–speed characteristics of an SRM.

from the motor. As the speed increases, the motional emf increases forcing the advancement of the current turn-on angle to obtain a maximum average torque. Current can still be control using pulsewidth modulation (PWM) or a hysteresis type current regulator.

When the speed increases further, the motional emf exceeds the dc bus voltage, and the motor operates in the single pulse mode. In this mode, the current is limited by the motional emf and never reaches the rated current. Hence current control is not possible, and the torque is maintained at the optimal by controlling only the turn-on and turn-off angle, in other words by controlling the conduction interval called as the dwell angle. In this region, the torque is inversely proportional to the speed and is called the constant power region.

The maximum value of the dwell angle is limited to half the rotor pole pitch beyond which the conduction becomes continuous. This is a natural region where the torque is controlled only by the natural characteristics and is inversely proportional to the speed.

BASICS OF SRM CONTROL

The basic control strategy involves switching the stator current during the rising inductance region of operation. The basic control variables include the turn-on angle, turn-off angle, and supply current. Additionally, however, depending on the mode of operation, there might be additional control variables; for example, in a hysteresis type current control the hysteresis band width can be an additional control variable.

Furthermore, in the low-speed region (below base speed) where the motion back-emf is not enough to distort the current waveform, current control is necessary to maintain a flat-topped current. Hysteresis control can be used for this purpose. In hysteresis-type of current control, the chopping band has to be optimally chosen as there is a tradeoff between the chopping frequency and the width of the band. Assuming the band has been optimally chosen, the maximum torque per ampere can be obtained by tuning the turn-on angle (θ_{on}) and turn-off angle (θ_{off}) of the phase current excitation.

It must also be noted that in the high-speed region both control angles are important. Indeed, turn-on angle has a very significant role for phase advancing as there, the current has to meet its maximum value at maximum torque point. It is also important to remember that in the high-speed region, current has a single pulse shape [see Fig. 8(c)] and there is no control on the shape of the current. Hence, one has to tune both turn-on angle and turn-off angle to obtain the maximum torque.

BASIC DESIGN OF SRM

Basic Machine Design

The machine design process involves finding a suitable set of machine dimension variables to satisfy a set of performance requirements taking into account minimization of cost, weight, and the like (see Fig. 8). The simple structure of the SR machine disguises the complex nature of the procedure required for its design. The inherent nonlinear nature of the SRM and its converter circuits and the relatively small body of knowledge on modeling and practical performance make the design procedure of SRM very difficult (5). The basic design parameters include the number of rotor poles, number of phases, pole arc to pole pitch ratio, and winding connections, among other things. Factors like switching frequency, core losses and flux distribution play an important role in the design of SRM. Figure 9 shows the design procedure for the SRM drive. The various steps of this flowchart will be briefly discussed in this section.

Determination of Initial Geometry

Number of Poles and Pole Arcs. The following factors must be taken into account in deciding the number of poles:

- minimization of mutual inductance between phases,
- self-starting capability at any rotor position and in either direction,
- minimization of the permeance at the unaligned position, and
- minimizing the switching frequency.

It can be shown that to satisfy these four requirements, the following equations should also be satisfied:

$$\mathrm{LCM}(N_s, N_r) = qN_r \tag{8}$$

and

$$\mathrm{LCM}(N_s, N_r) > N_s > N_r \tag{9}$$

where N_s and N_r are even, q is greater than 2, and LCM denotes the least common multiple operation. For pole arcs,

$$\min(b_r, b_s) > \frac{2p}{qN_r} \tag{10}$$

and

$$\beta_s \le \frac{2\pi}{qN_r} - \beta_r \tag{11}$$

Based on these conditions, optimal number of poles and pole arcs can be obtained for different types of application require-

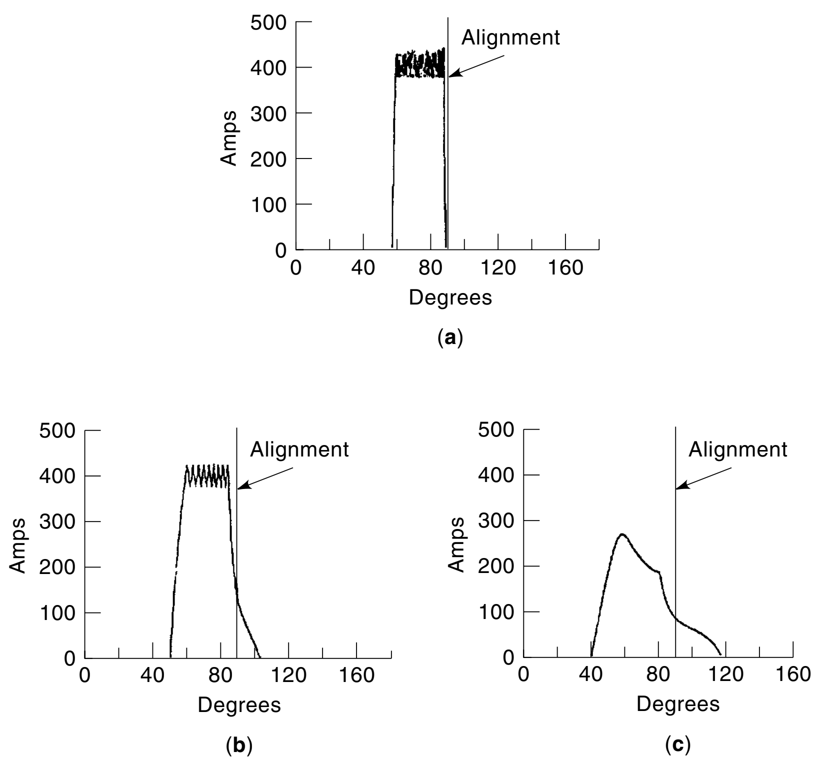

Figure 8. Currents in different modes. (a) Low-speed motoring, (b) medium-speed motoring, and (c) high-speed motoring.

ments. Because there are qN_r steps per revolution, the step angle is given by

$$\theta_s = \frac{2\pi}{qN_r} \tag{12}$$

Switching Frequency. The switching frequency is directly dependent on the number of phases as given by

$$f = \frac{qN_r\omega}{2\pi} \tag{13}$$

Because the core loss and switching losses in the converter circuit increase with frequency, the number of phases must be chosen based on the preceding factor considering applications requiring high efficiency. However, for low-speed applications, switching frequency or the number of phases is not a limiting factor.

Number of Phases. The required starting torque greatly influences the choice of the number of phases. The number of phases must be chosen in such a way that there is enough overlap between the inductance variation of any two adjacent phases. Accordingly, a four-phase machine offers much flexibility in terms of starting performance compared to a three-phase machine.

The stator–rotor pole combinations can be decided, again, based on the performance requirement. Typical combinations include 8–6 and 6–4. If a combination of 4–2 or 2–2 is chosen, then the starting torque will be zero if the poles are aligned. In SRMs with stator phases greater than three, at least one phase is not energized at any instant, possibly for indirect position sensing. (See discussion in a later section.) Furthermore, a multiple number of poles per phase can be considered in selecting stator–rotor pole combinations. In fact, by increasing the number of poles per phase, one can achieve high starting torque and less torque ripple while the same amount of silicon corresponding to one pole per phase configuration is being used. Figure 10 depicts the cross section of a 12/8 three-phase SRM. However, it must be noted that by using such configurations higher mutual coupling between phases is expected.

Stator and Rotor Outer Diameter. Geometrical constraints are often given in terms of the length or outer diameter of the machine. A designer has to make a compromise between these two parameters. Reduction in the generated torque due to ending effects in the pancake-type (length of the machine is less than its outer diameter) SRM is the main disadvantage for choosing machines with short length and large diameters. On the other hand, very long machines are subject to cooling difficulties.

The electromagnetic torque developed by the SRM depends mainly on the outer diameter and the available ampere turn in the coils, as follows:

$$T \propto D_r^2 (Ni)^2 \tag{14}$$

where D_r and Ni denote rotor outer diameter and ampere turn, respectively. According to this expression, in order to obtain the maximum torque, rotor diameter and ampere turn have to be maximized. However, increasing the rotor diameter results in reduction of the space available for coils. Therefore, as an initial value, rotor diameter is set to stator outer radius. Moreover, it must be noted that the moment of inertia of the machine depends on the rotor diameter. Therefore, if

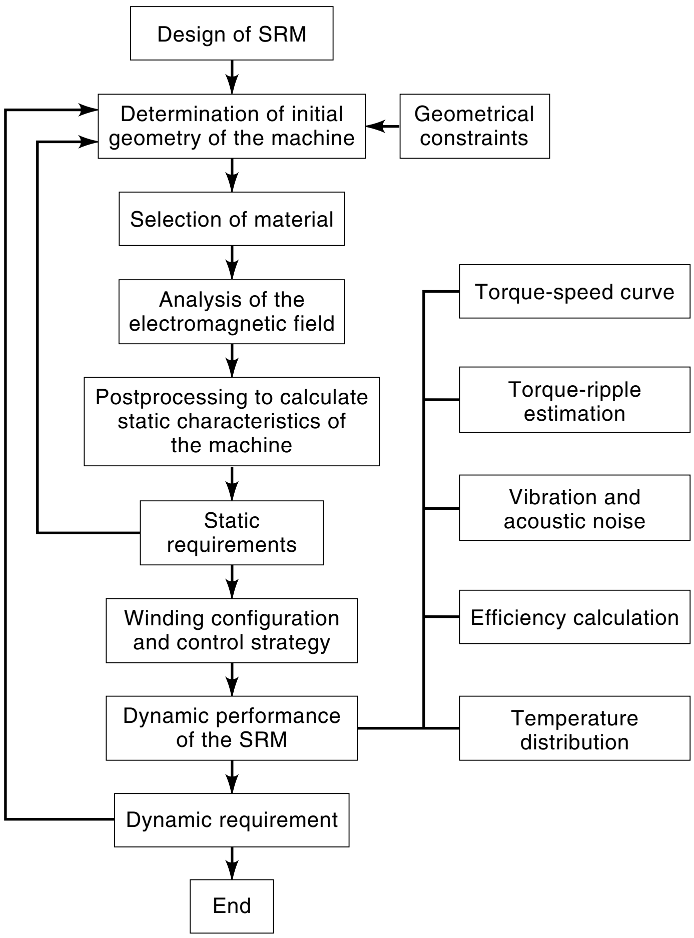

Figure 9. Design procedure for SRM drive.

dynamic response of the system has to meet certain requirements, an optimization for the rotor diameter has to be performed.

Material Selection and Winding Configuration. The SRM can be built using commercially available steel laminations such as M-19 and M-45. Magnetization curve of the steel being used for manufacturing the SRM enhances the efficiency of the drive. Level of saturation as well as losses per unit of mass should be considered for selecting the appropriate material.

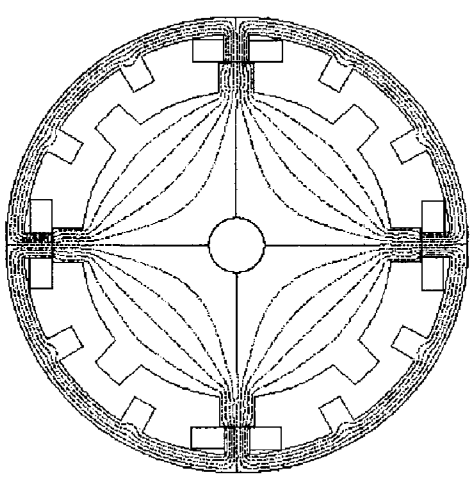

Figure 10. Flux lines of a 12/8 SRM at aligned position.

Regarding the windings, since concentrated windings are used in the SRM structure, once the total ampere turn in the coils is determined, one can perform dynamic simulation of the drive using a reasonable number of turns. By choosing the base speed, the required motion back-emf is calculated and so is the exact number of turns per winding.

A more detailed explanation regarding the selection of other parameters such as airgap, stator–rotor pole length, and shaft diameter can be found in Ref. 7.

In order to calculate machine parameters such as inductance profile and static torque characteristics under saturation, finite element or boundary element methods are used. Figure 10 shows an example of flux lines obtained using a finite element method for a 12/8 SRM configuration. Indeed, double saliency and saturated magnetic path in the SRM are the main motivations for performing numerical analysis of the machine.

It must be mentioned that because of a very narrow airgap and double saliency of the machine structure, numerical analysis of the SRM is not trivial and special considerations have to be taken into account. Some of the methods used for computing machine characteristics, which are functions of rotor position and stator current, are listed here:

1. Maxwell stress method
2. Energy method
3. Virtual work method

Discussion of the details of these algorithms is beyond the scope of this article. Interested readers are referred to Ref. 7.

Basic Converter Design

SRMs cannot operate directly with a dc supply or the standard sinusoidal ac supply available off the wall. Hence, the converter must be designed so that it is coordinated concurrently with the design of the motor to obtain an optimal design of the drive as a whole. Unlike the motors that operate with sinusoidal voltages and currents, the converter topology in an SRM is dependent on the machine design. The topology depends on the motor configuration, number of stator and rotor poles, and associated conduction and overlap angle (8). In general, the starting torque requirements decide the current rating, and the maximum speed of the motor decides the voltage rating of the inverter. The different converter topologies are shown Fig. 11. Note that a number of new topologies such as soft-switched and improved C-dumped converters have recently been developed and are not included in Fig. 11.

An ideal converter must satisfy

- low switches per phase ratio
- ability to supply and control a commanded current independently and precisely
- flexibility in adapting to any number of phases (odd or even)
- low VA rating for a given rating of the drive
- robustness and reliability

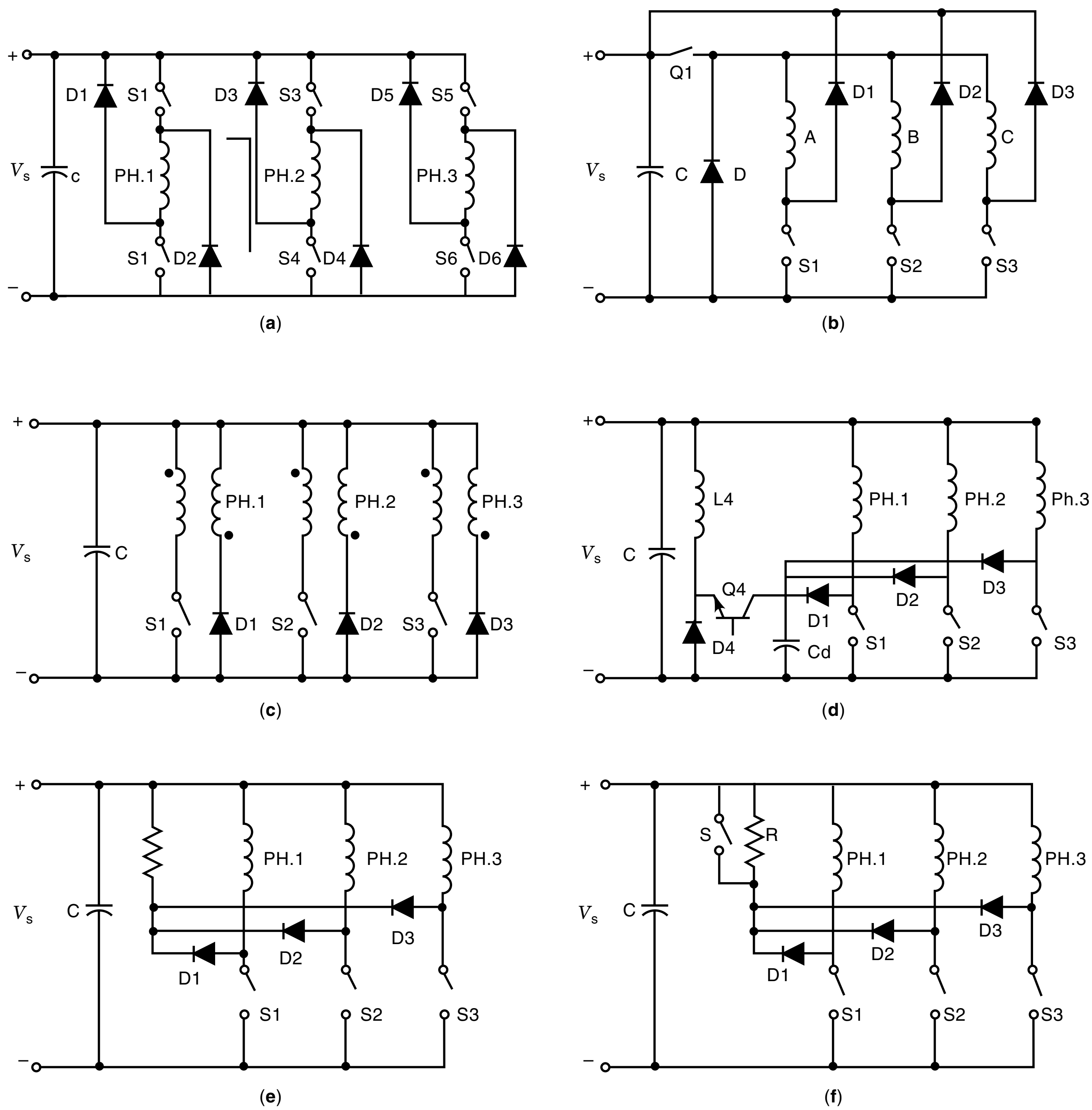

Figure 11. SRM converter topologies. (a) Classic converter, (b) (n + 1) switch converter, (c) bifiliar winding converter, (d) C-dump converter, (e) suppression resistor converter, and (f) dual decay converter.

- good efficiency
- ability to operate in all four quadrants effectively
- less torque ripple and noise

The most commonly used converter types are the classic half-bridge converter and the split-phase converter. The classic converter is the most flexible type of converter, but it requires more switches. The splits phase converter requires an even number of phases and has a high active device rating; hence, it is suitable only for low-voltage and low-power applications. Another type of converter suitable for a star-connected SRM is the dual-decay converter with flexibility of control in freewheeling mode and reduced device ratings (9). Most of the converters developed recently are aimed at reducing the number of switches and are more application specific.

METHODS OF CONTROL WITH SENSOR

Because the basic control strategy in an SRM involves properly placing the current pulses at the positive torque-producing region of inductance variation for optimum torque production, most of the SRDs are on position sensors feedback. From

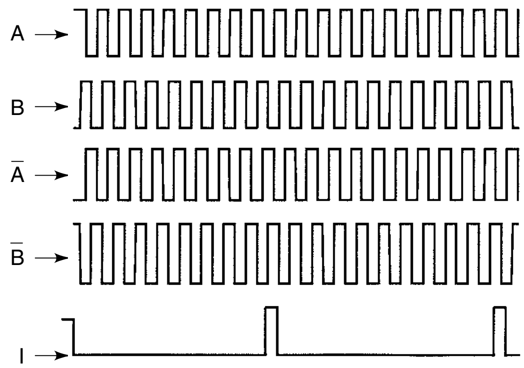

Figure 12. Sensor waveforms for forward rotation.

the torque Eq. (7), even though it neglects saturation, we can see that the optimum torque is obtained when the current pulse is placed only during the positive slope of the inductance region. Note that this assumption is not valid under high-speed saturated condition.

In the motoring operation, the current pulse is established during the positive slope of the inductance profile (10). For low-speed operation, the current is limited by chopping or PWM control, and current is turned off such that the current does not extend much into the negative slope region of the inductance profile so as to limit the negative torque produced to the minimum possible level.

Position Sensing Requirements

The angle information is usually obtained from a high-resolution resolver. Optical encoders and inductive and Hall effect sensors also can be used. Figure 12 shows a typical pulse output of the optical encoders for the forward rotation. In this figure A and B denote the quadrature pulses generated by an optical encoder. In addition, the complementary outputs (A, B) and the index pulse (I) are shown and can be used for control purposes. These pulses can be used to program a counter (in the processor) which provides position information required in the control. It must be noted that angle sensitivity has to be high at high speeds. Also, servo applications demand a high-resolution position sensor. For high-speed operation, a phase-locked loop can be used to synchronize high-frequency pulse train to the sensor output for good resolution.

SRMs can be fed either by current source (CS) or by voltage source (VS) (11,12). A CS supply-based SRM includes a current source of variable amplitude and a power converter. In this the suitable strategy will be to fix the turn-on and turn-off angles and to vary the current amplitude for the control of the motor. One advantage of this method is that the motor torque is directly proportional to the control variable (i.e., current amplitude). The most commonly used SRM drive system is fed by voltage source. This drive consists of a VS supply, a current feedback loop, and the necessary control circuitry. This drive has different control variables based on the different modes of operation. They offer a better torque capability than the current source switched reluctance motor (CSSRM).

SENSORLESS OPERATION

Closed-loop operation of a reluctance motor requires rotor position information for satisfactory performance. Conventional methods used for position sensing include resolvers, inductive or Hall effect sensors, and optical encoders. These methods have such disadvantages as additional cost, additional electric connections, mechanical alignment problem, and less suitability to space restricted application, in addition to the significant disadvantage of being a potential source of unreliability. These lead to the research in sensorless operation of reluctance motors, resulting in several techniques in the past two decades. Most of the existing methods extract the rotor position information from the measurable electrical parameters. These techniques eliminate the requirement of the conventional position sensors, thereby increasing the reliability of the motor drive system considerably. They can be classified as

1. Active probing methods
   a. Linear relation methods
   b. Inverse relation methods
2. Nonintrusive methods
3. Open loop methods
4. Other methods

Active Probing Methods

The active probing methods use the responses of diagnostic signals injected into the passive (unenergized) phase of an SRM. These methods are suitable for low speeds as the time window for passive phase measurement reduces at high speeds. Usually, the phase to be energized next is diagnosed for position estimation. They can be further classified as linear relation methods and inverse relation methods.

Linear Relation Methods. In linear relation methods, the signal containing position information is directly proportional to the phase inductance. In a typical method, the rate of change of phase current, which is influenced by the incremental inductance, is monitored (13). Rotor position can now be deduced because the incremental inductance is a function of rotor position. This has an advantage of deducing the rotor position even at zero speed. Another method, called the PM encoder technique, is robust to switching noise and was presented in Ref. 14. A sinusoidal carrier voltage signal of frequency much higher than that of the frequency of variation of inductance is chosen. Thus, the transient variation of the current phase will contain the information about the dynamic motor winding inductance. This encoded inductance information is decoded using zero-crossing detectors for the voltage and current. The demodulator generates a square wave signal whose pulse width variation represents the phase inductance variation.

The phase angle is given by

$$\phi = \tan^{-1}\frac{\omega L}{R} \tag{15}$$

The detected inductance is given by

$$L = \frac{R\tan\phi}{\omega} \tag{16}$$

Also a modified PM encoder technique suitable for a wide range of speeds is presented. Mathematical analysis and simulation results show that the PM technique is more sensitive for lower values of inductance and the amplitude modulation (AM) technique is more sensitive for higher inductance values. To achieve a better sensitivity, a level-crossing detector is used instead of a zero-crossing detector. The level-crossing detector is set to a threshold value. Now the square wave output corresponds to the phase angle variation with respect to the threshold value other than zero. It gives better sensitivity than the PM method.

Inverse Relation Methods. In the inverse relation methods, the position information encoded signals are inversely proportional to the phase inductance. At high speeds, the motional emf is very high, and the current will never reach the rated value resulting in a single pulse mode. In this mode, the current gradient in the next phase to be excited has the position information (13). At the turn-on position, because the resistive voltage drop and the motional emf are negligible, the initial rate of change of current is given by

$$\left.\frac{di}{dt}\right|_{i=0} = \frac{v}{l} \tag{17}$$

Therefore the di/dt is inversely proportional to the incremental inductance; consequently, the position information in the preceding equation is at low phase currents. The sensorless operation is implemented by comparing the initial current gradient with a optimal current gradient. In the amplitude modulation method (15,16), the position information can be obtained from the amplitude of the current because it is directly proportional to the inductance variation. In this method, the envelope of the modulated current signal is detected. In addition, the information can be decoded by measuring the amplitude in terms of angles using a level crossing detector.

Nonintrusive Methods

In the nonintrusive methods, the rotor position is obtained based on the measurable parameters without using any diagnostic or probing signals. Neglecting R, at low speeds the incremental inductance $l = d\psi/di$ is a function of θ for constant i. Therefore, dt, rise time or fall time, can be used to obtain the position information. The flux linkage curve information on a multidimensional look-up table can be used to determine rotor position (17,18). In another method called the active phase vector method (19), a composite vector, which is directly proportional to the inductance, is obtained based on the discrete form of voltage equation for different modes of operation. Active phase vector methods are computationally less intensive and digital implementation is easy.

Open Loop or Synchronous Control Method

These methods are based on synchronous control and do not actually provide any position information. The motor is run from a variable frequency oscillator, and change is made only to the dwell angle to improve the stability (20).

Other Methods

Observer Based. The observer method reconstructs the state of the SRM drive system on the basis of known system inputs and system measurements (21). Measurements of input voltages and currents were used. An accurate mathematical model including mechanical load (in state space form) to estimate current, flux linkage, speed and rotor position which was compared with actual current and error adjustment made using an adjustment matrix to estimate the position is used.

Mutually Induced Voltage-Based Methods. In this method, the mutually induced voltage in an unenergized phase caused by current in an energized phase is monitored to obtain the position information (22).

Design-Based Method. The design-based method is based on altering slightly the structure of at least one of stator and/or rotor pole faces, which will introduce a perturbation in the inductance profile of the motor while it is running (23). The perturbations can be produced by introducing a notch or bump in the stator and/or rotor pole faces. The frequency of these perturbations gives a direct information on the speed of the motor.

Sliding Mode Observer-Based Controllers. This method utilizes estimated rotor position obtained from an observer for purposes of electronic commutation of machine phases. A more detailed explanation of this technique can be found in Ref. 38.

OVERVIEW OF CRITICAL ISSUES

Apart from the numerous advantages, SRMs are also known for their high torque pulsations, high acoustic noise, and reliability issues resulting from sensor-based operation.

Torque Ripple

The nonlinear coupling between the rotor position, phase current, and overlap angle and the doubly salient geometric structure of the SRM are the intrinsic causes of torque ripple in a SRM. Torque ripple is very undesirable in low-speed and servo type applications. Several methods have been developed to reduce torque ripple based on machine design or control strategies.

Design-Based Methods. Torque ripple can be minimized by suitably designing the magnetic structure of the machine (24). Comprehensive procedures, beginning with the fundamental selection of pole numbers and geometry, for designing SRM drives for low-torque-ripple applications has been presented in the literature (25). Values for specific torque are used to estimate the required SRM size and are obtained from empirical data or from an analytical estimation method. Pole numbers are chosen based on the speed and torque ripple specifications for the design. The pole numbers define a range of feasible pole arc combinations. The center pole arc values are chosen as a starting point. The current density in the phase winding is also chosen based on the thermal constraint of the application. The pole arcs and motor dimensions that yield minimum ripple are selected as the candidate design, which is further evaluated using the dynamic SRM model.

Control-Based Methods. Classical linear controllers cannot eliminate the torque pulsations. The fundamental approach is by optimal current profiling that reduces torque pulsations. Torque ripple can be reduced by using a current-tracking control method in which the desired stator currents are computed by linearizing and decoupling transformation (26). The shape of static torque–angle–current characteristics of SRM drive can be fully determined by a series of measurements performed with the drive in a self-learning mode (27). Based on this, the current required to obtain the optimum torque contribution from each phase, at each rotor position, can be determined for a smooth torque performance. A single input, linear, decoupled output torque controller based on optimal precalculation of the phase current profile provides low torque ripple (28). A bicubic spline interpolation was used to model the nonlinear experimental data. This method optimizes the current overlap at all torque levels so as to minimize the peak phase current. This current profiling algorithm results in the highest possible operating speed range under constant torque operation. The torque output is decoupled single-input linear function of torque input demand. Neural techniques can learn the current profiles required to minimize torque ripple and to satisfy other performance criteria on-line (29). Torque measurement is required to train the neural network. PWM current control can be used for smooth operation of an SRM drive (30). The torque pulsations during commutation are minimized by a current control strategy that allows simultaneous conduction of two positive torque producing phases over an extended predefined region. The effects of saturation can also be taken into account. Furthermore, intelligent algorithms can be employed to achieve minimum torque ripple of the SRM drive. Recently, fuzzy logic-based controllers, neural networks, and neuro-fuzzy techniques have been successfully used for this purpose (39–41).

Acoustic Noise

Acoustic noise in SRMs is at a relatively higher level when compared to other ac drives. The acoustic noise has both magnetic and mechanical origin (31). The possible sources include radial attractive forces between the rotor and stator, stator vibrations induced by the torque ripple, stator winding vibrations induced by the interaction of the stator current and the local magnetic field, magnetostrictive forces in the stator laminations, and unbalanced magnetic and mechanical forces on the rotor as a result of manufacturing asymmetry windage and bearing vibrations. Of these, the dominant one is shown to be the radial attraction force between rotor and stator poles. In fact, avoidance of a resonance in radial and tortional vibration of the stator and rotor can reduce acoustic noise (42). Acoustic noise can be reduced by current shaping or by introducing dither into the turn-on and turn-off angles. In another technique, a chopper is introduced between rectifier and converter to reduce the phase voltage with respect to the speed (32). The voltage-smoothing method reduces the rate of change of radial force and produces a smaller vibration (33). Also described in the literature is a three-stage commutation technique that cancels the stator vibrations when the power converter does not have a 0 V loop by employing the three-stage commutation technique at the beginning and end of the 0 V loop. The active cancellation methods like the three-stage commutation technique are superior to the voltage-smoothing method because they allow the energy to be dissipated in subsequent vibrations that can completely oppose each other. Research in this area is still in the infant stage, and further developments are expected in the near future.

Sensorless Operation

A trade-off exists between extensive computation and good resolution in position sensing. There is still a lot of room for improvement because no accurate, commercially applicable methods are available. The need for inexpensive, reliable, indirect position-sensing technique for a wide range of speeds still exists. The advances made in the fields of power electronics, motion control, and signal processing can be used to improve the commercial applicability of the existing methods. The existing computationally intensive, high-resolution sensorless techniques can be made commercially viable in the future with the advances made in the computational power of digital signal processors.

Need for Self-Tuning. The following assumptions (34) are made in most of the conventional sensorless methods:

- The inductance is symmetrical about the aligned position.
- All the rotor and stator poles have perfect symmetrical tooth structures.
- The inductance variation is time and temperature independent.
- Saturation has no or very little effect on the inductance variation.
- The inductance profile is identical for all the phases.
- The inductance profile is identical for all the machines of the same rating in mass production.

In practice, these assumptions are not valid, and these factors affect the sensitivity of a sensorless algorithm. Sensorless methods that can adapt to the parameter drifts are required to optimize the machine performance. The corruption of position information resulting from the secondary effects of the existing sensorless methods must be considered to improve accuracy. Further development resulting in commercially applicable, inexpensive techniques is expected. Need for an inexpensive, indirect position-sensing technique suitable for high-speed applications still exists. More research will be necessary for a method with good positional accuracy that is suitable for commercial application.

ADVANCED CONTROL SCHEMES

A reliable drive system has the following characteristics:

- parameter insensitive control characteristics,
- quick precise dynamic response with no overshoot, and
- rapid recovery from transient disturbances.

Conventional linear controllers are quite sensitive to plant parameters. This along with the need for optimum performance of SRM like maximum efficiency, maximum torque, and minimum torque ripple calls for sophisticated control strategy. The important control parameters in an SRM (switch-on and switch-off angles) are a nonlinear complex function of many motor parameters; consequently, they re-

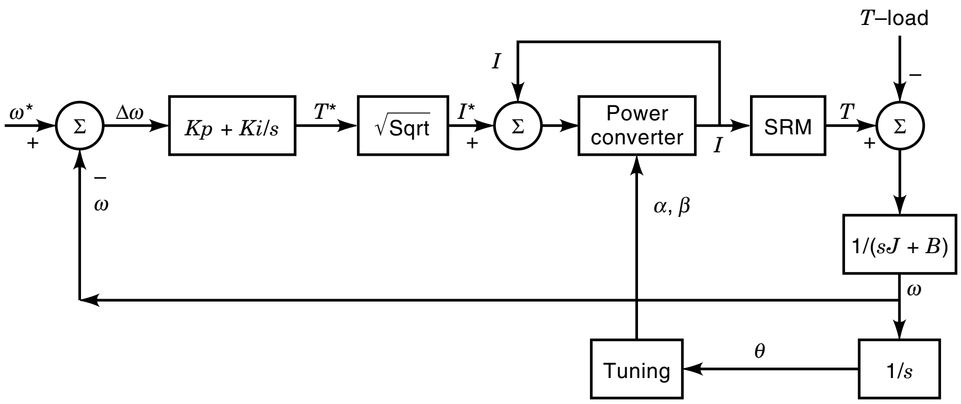

Figure 13. Control block diagram with self-tuning algorithm.

quire fine tuning (sophisticated control) for optimal performance. The advanced control strategies developed in the recent years include sliding mode control, artificial neural networks and fuzzy-logic-based control, and self-tuning control. In a sliding mode control, the states of the system is forced to slide on a given sliding surface in the state space. These methods are shown to provide a better torque ripple characteristics and are insensitive to parameter variations and disturbances. Artificial neural networks (ANNs) have been used successfully in the control of nonlinear dynamic systems (29). The capability to accommodate accurate nonlinear modeling has made ANNs ideal candidates for solving the control strategies of inherently nonlinear SRMs. Fuzzy logic controllers are gaining interest recently in the field of nonlinear control (35). They offer the following advantages:

- It does not require an accurate model of the plant.
- It can be designed on the basis of linguistic information obtained from the previous knowledge of the control of the machine.
- Fuzzy logic controllers gives better performance results than the conventional controllers.

Recently the problem of obtaining optimal performance from an SRM in the presence of parameter variation has gained considerable interest recently (36). New self-tuning algorithms that optimize the steady-state performance of the drive as measured by torque per ampere (TPA) have been introduced, but only recently have we discovered that the phase inductance profiles can significantly differ from the design data as a result of parameter variation and drift (34). So, it becomes necessary to use a controller with self-tuning capability if optimal performance of the SRM drive is to be maintained. Maximum TPA is desirable for any drive application because the motor may be described as a current to torque transducer. Specifically, the following problems arise in practical SRMs:

- Because of manufacturing tolerances, the inductance profile varies by as much as 10% from phase to phase of the motor (36) and also from motor to motor with the same design and rating. Note that the minimum inductance does not show any significant variation because of the very large air-gap at the unaligned position. However, the maximum inductance occurs at the aligned position where the air gap may be less than 1 mm. So, any minor variations in the air-gap show up in the maximum inductance. Thus, the slope of the inductance profiles will also differ, and the torque production will be affected.
- With time, there will be wear on the bearings; consequently, the air-gap may change or acquire a small eccentricity. Again, this has an impact on the maximum inductance of each phase.

Hence, the optimal values of the turn angle calculated off-line are sufficient for the TPA maximization. An on-line, self-tuning algorithm to determine the optimal value of the turn-off angle in the presence of parameter variations which alter the inductance profiles has proven to produce superior steady-state performance. Figure 13 shows the block diagram of this particular self-tuning control.

The inherent simplicity of this new approach makes it ideal for real-time implementation in a digital control system. The control scheme is applicable to any SRM drive operated with a shaft position sensor, and does not depend on the number of phases, poles, or HP of the motor.

APPLICATIONS

SRMs have been successfully applied to a variety of applications resulting in high-performance drives. Figure 14 shows the typical efficiency vs. speed for curves for various 30 hp motors. The first successful applications were as general-pur-

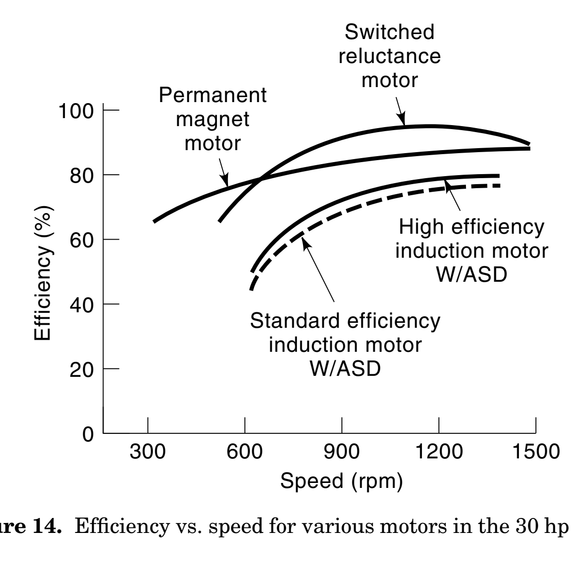

Figure 14. Efficiency vs. speed for various motors in the 30 hp range.

pose industrial drives. Good fault tolerance and the ability to operate in harsh environments made SRMs successful candidates as coal-shearing machine, textile spinning drive, friction welding machine, food processor applications, plotters, and aerospace and automotive applications. SRMs of 5 MW at 50 rpm to 10 kW at 100,000 rpm have been built and tested successfully. Moreover, low-cost and high-performance attributes make SRMs alternatives for many applications below 10 hp. Also, SRMs have a very wide speed range, defined as the ratio of maximum speed in the constant power region to the base speed (where motional back-emf equals the terminal voltage). With use of a proper control strategy (43), a speed ratio of 6 : 1 is achievable.

The fault tolerance capability of SRMs is extremely good, making SRMs suitable for aerospace, automotive, and industrial applications. The independence of each phase windings and the absence of shoot-through paths contributes to the fault tolerance of the SRMs. Typical applications include traction, domestic appliances, mining, servo type, and battery-powered applications. The application areas of SRM are rapidly expanding because SRMs can compete virtually in any industrial or domestic drive market.

BIBLIOGRAPHY

1. P. J. Lawrenson, Switched reluctance drives: A perspective, *Proc. Int. Conf. Electr. Mach.,* vol. 1, 1992, pp. 12–21.
2. Bedford, *Compatible permanent magnet or reluctance brushless motors and controlled switch circuits,* U.S. Patent No. 3,678,352, 1972.
3. Bedford, *Compatible brushless reluctance motors and controlled switch circuits,* U.S. Patent No. 3,679,953, 1972.
4. W. F. Ray and R. M. Davis, Inverter drive for doubly-salient reluctance motor: Its fundamental behavior, linear analysis and cost implications, *IEE Elec. Power Appl.,* **2** (6): 185–193, 1979.
5. P. J. Lawrenson et al., Variable speed switched reluctance motors, *IEE Proc, Part B,* **127** (4): 253–265, 1980.
6. R. M. Davis, W. F. Ray, and R. J. Blake, Inverter drive for switched reluctance: Circuits and component ratings, *IEE Proc., Part B,* **128** (2): 126–136, 1981.
7. J. E. Miller (ed.), *Switched Reluctance Motor Drives,* Ventura, CA: Intertec Commun., 1988.
8. S. Vukosavic and V. R. Stefanovic, SRM inverter topologies: A comparative evaluation, *IEEE Trans. Ind. Appl.,* **27**: 1034–1047, 1991.
9. M. Ehsani et al., Dual-decay converter for switched reluctance motor drives in low-voltage applications, *IEEE Trans. Power Electron.,* **8**: 224–230, 1993.
10. B. K. Bose et al., Microcomputer control of switched reluctance motor, *IEEE Trans. Ind. Appl.,* **22**: 708–715, 1986.
11. G. S. Buja and M. I. Valla, Control characteristics of the SRM drives. Part I. Operation in the linear region *IEEE Trans. Ind. Electron.,* **38**: 313–321, 1991.
12. G. S. Buja and M. I. Valla, Control characteristics of the SRM drives. Part II. Operation in the saturated region, *IEEE Trans. Ind. Electron.,* **41**: 316–325, 1994.
13. P. P. Acarnley, R. J. Hill, and C. W. Hooper, Detection of rotor position in stepping and switched motors by monitoring oc current waveforms, *IEEE Trans. Ind. Electron.,* **32**: 215–222, 1985.
14. M. Ehsani et al., New modulation encoding techniques for indirect rotor position sensing in switched reluctance motors, *IEEE Trans. Ind. Appl.,* **30**: 85–91, 1994.
15. M. Ehsani, I. Hussain, and A. B. Kulkarni, Elimination of discrete position sensor and current sensor in switched reluctance motor drives, *IEEE Ind. Appl. Soc. Conf. Proc.,* 1990, pp. 518–524.
16. M. Ehsani, *Position sensor elimination technique for the switched reluctance motor drive,* U.S. Patent No. 5,072,166, 1991.
17. B. G. Hedland, *A method and a device for sensorless control of a reluctance motor,* Int. Patent No. WO 91/02401, 1986.
18. B. G. Hedlund, *Method and a device for sensorless control of a reluctance motor,* U.S. Patent No. 5,173,650, 1992.
19. M. Ehsani and K. R. Ramani, New commutation methods in switched reluctance motors based on active phase vectors, *IEEE Power Electron. Specialists Conf. Rec.,* 1994, pp. 493–499.
20. J. E. Miller, J. T. Bass, and M. Ehsani, Stabilization of variable-reluctance motor drives operating without shaft position sensor feedback, *Incremental Motion Control Syst. Devices Proc.,* 1985, pp. 361–368.
21. A. Lumsdaine and J. H. Lang, State observers for variable-reluctance motors, *IEEE Trans. Ind. Electron.,* **37**: 133–142, 1990.
22. I. Hussain and M. Ehsani, Rotor position sensing in switched reluctance motor drives by measuring mutually induced voltages, *IEEE Trans. Ind. Appl.,* **30**: 665–672, 1994.
23. R. P. Bartos, T. H. Houle, and J. H. Johnson, *Switched reluctance motor with sensorless position detection,* U.S. Patent No. 5,256,923, 1993.
24. Byrne, M. F. McMullin, and J. B. O'Dwyer, A high performance variable reluctance drive: A new brushless servo, *Proc. Motorcon Conf.,* Chicago, IL, 1985, pp. 139–146.
25. D. P. Tormey and D. A. Torrey, A comprehensive design procedure for low torque-ripple variable-reluctance motor drives, *IEEE Ind. Appl. Soc. Annu. Meeting,* 1991, pp. 244–251.
26. Wallace and D. G. Taylor, Three-phase switched reluctance motor design to reduce torque ripple, *Proc. Int. Conf. Elect. Mach.,* Cambridge, MA, 1990, pp. 783–787.
27. R. C. Kavanagh, J. M. D. Murphy, and M. G. Egan, Torque ripple minimization in switched reluctance drives using self-learning techniques, *IEEE Ind. Electron. Conf.,* 1991, pp. 289–294.
28. D. S. Schramm, B. W. Williams, and T. C. Green, Torque ripple reduction of switched reluctance motors by phase current optimal profiling, *IEEE Power Electron. Specialists Conf.,* 1992, pp. 856–860.
29. D. S. Reay, T. C. Green, and B. W. Williams, Neural networks used for torque ripple minimization from a switched reluctance motor, *5th Eur. Conf. Power Electron. Appl.,* vol. 6, 1993, pp. 1–6.
30. I. Hussain and M. Ehsani, Torque ripple minimization in switched reluctance motor drives by PWM current control, *IEEE APEC,* 1994, pp. 72–77.
31. D. E. Cameron, The origin and reduction of acoustic noise in doubly salient variable-reluctance motors, *IEEE Trans. Ind. Appl.,* **28**: 1250–1255, 1992.
32. P. Pillay et al., A chopper-controlled SRM drive for reduced acoustic noise and improved ride-through capability using super capacitors, *IEEE Ind. Appl. Soc. Conf. Rec.,* 1994, pp. 313–321.
33. C. Pollock and C. Y. Wu, Acoustic noise cancellation techniques for switched reluctance drives, *IEEE Ind. Appl. Soc. Conf. Rec.,* 1995, pp. 448–455.
34. M. Ehsani and K. R. Ramani, Direct control strategies based on sensing inductance in switched reluctance motors, *IEEE PESC Rec.,* 1993, pp. 10–16.
35. S. Bolognani and M. Zigliotto, Fuzzy logic control of a switched reluctance motor drive, *IEE IAS Conf. Rec.,* 1993, pp. 2049–2054.
36. P. Tandon, A. V. Rajarathnam, and M. Ehsani, Self-tuning control of a switched reluctance motor drive with shaft position sensor, *IEEE Trans. Ind. Appl.,* **33**: 1002–1010, 1997.
37. M. Ehsani et al., Sensorless control of switched reluctance motors: A technology ready for applications, *ICEM Conf. Rec.,* 1998.

38. I. Husain, S. Sodhi, and M. Ehsani, A sliding mode observer based controller for switched reluctance motor drives, *IEEE Ind. Appl. Soc. Conf. Rec.,* 1994, pp. 635–643.
39. D. S. Reay et al., Fuzzy adaptive systems applied to the control of a switched reluctance motor, *IEEE Int. Symp. Intelligent Control, Conf. Rec.,* 1994, pp. 81–86.
40. J. G. O'Donovan et al., Neural network based torque ripple minimization in a switched reluctance motor, *IEEE Ind. Appl. Soc. Conf. Rec.,* 1994, pp. 1226–1231.
41. C. Rochford et al., Development of smooth torque in switched reluctance motors using self-learning techniques, *EPE Conf. Rec.,* 1993, pp. 14–19.
42. B. Fahimi et al., Mitigation of acoustic noise and vibration in switched reluctance motor drives using neural network based current profiling, *IEEE Ind. Appl. Soc. Conf. Rec.,* 1998.
43. K. M. Rahman et al., Advantages of switched reluctance motor applications to EV and HEV: Design and control issues, *IEEE Ind. Appl. Soc. Conf. Rec.,* 1998.

MEHRDAD EHSANI
B. FAHIMI
Texas A&M University

SWITCHES, ELECTRO-OPTICAL. See ELECTRO-OPTICAL DEVICES; ELECTRO-OPTICAL SWITCHES.

SWITCHES, PHOTOCONDUCTING. See PHOTOCONDUCTING SWITCHES.

SWITCHES, VACUUM. See VACUUM SWITCHES.